

A novel dual-lens-coupling system for DFB laser based on hybrid integration*

WEI Juan (魏娟)^{1,2,3}, SUN Yu (孙瑜)^{1,3**}, XUE Haiyun (薛海韵)^{1,3}, HE Huimin (何慧敏)^{1,3}, SUN Siwei (孙思维)^{1,3}, LIU Fengman (刘丰满)^{1,3**}, and CAO Liqiang (曹立强)^{1,3}

1. System Packaging and Integration Research Center, Institute of Microelectronics of Chinese Academy of Sciences, Beijing 100029, China

2. University of Chinese Academy of Sciences, Beijing 100059, China

3. National Center for Advanced Packaging, Wuxi 214028, China

(Received 13 September 2020; Revised 14 October 2020)

©Tianjin University of Technology 2021

A dual-lens-integrated distributed feedback (DFB) laser based on hybrid integration for single-mode transmitter optical subassembly (TOSAs) is discussed in this paper. The alignment and fixing of the lenses are simple to manipulate and highly accurate, making it possible to achieve high-efficient optical coupling to single-mode fiber (SMF) without additional high-precision tools and fixing equipment. The capability for a low coupling loss of less than 3 dB between the laser and fiber was demonstrated. The fabricated TOSA module has clear opening eyes with minor time jitters at a bit rate of 25 Gbit/s. This hybrid integration is a low fabrication cost, compact, and low insertion loss method to manufacture TOSA for a 200 or 400 GbE optical transceiver in a high-speed optical network.

Document code: A **Article ID:** 1673-1905(2021)07-0395-5

DOI <https://doi.org/10.1007/s11801-021-0143-1>

In recent years, the increasing number of fiber access networks and the continuous rollout of 5G services are driving higher transmission rate and larger interconnection density which pose huge challenges to the current communication networks^[1]. Therefore, the appearance of optical interconnection has attracted great attention and has been applied widely in the telecommunication networks and data center networks. Distributed feedback (DFB) laser diode with narrower linewidth and higher output power has become a significant optical source for long-reach optical transmission by employing parallel fibers or wavelength division multiplexing (WDM) approach^[2]. With the development of small-form transceivers^[3], the optical sub-assembly, especially the optical coupling structure between DFB and optical elements in the transmitter optical subassembly (TOSAs) has become a critical part which has a non-negligible influence on power consumption and hybrid integration density of optical systems.

Generally, the TOSAs can be categorized as two types according to the optical coupling schemes: direct coupling^[4,5] and lens coupling^[6-8]. Direct coupling schemes require a submicron alignment tolerance and have a high coupling loss because of the significant mode mismatch between lasers and planar lightwave circuits (PLC) / single mode fibers (SMF). Although with the maturity of fiber micro-lens processing technology in recent years,

the coupling efficiency has been greatly improved, and the offset tolerance problem has been partially solved^[9-12]. However, the laser system with direct fiber coupling can only transmit in a single channel. Therefore, it is difficult to be applied in high-speed optical networks such as data centers or coherent optical communication on a large scale.

For lens coupling of DFB lasers, the main challenge and limitation are the alignment and fixing of different optical components because of their sub-micron positional tolerances, which means high-precision tools and fixing equipment are required to achieve efficient optical coupling. However, highly accurate tools are of large size and complicate, and require tight process control, so they are expensive for practical applications. Besides, the fixing methods using laser welding or solder/epoxy bonding often result in large offsets in post-bonding of optical components which will degrade device performance and reduce manufacturing yields^[13]. Researchers have made lots of efforts on improving coupling efficiency between DFB laser and optical elements. Previous solutions include the use of ball lenses or aspherical lenses, causing incident light rays to focus on different points when forming an image. The divergence angle of the laser and the size of the spot can be determined by the design of the lenses^[14,15]. In addition, to overcome time-consuming assembly process and high-precision requirements, an integration solu-

* This work has been supported by the National Key R&D Program of China (No.2017YFB0404800).

** E-mails: sunyu@ime.ac.cn; liufengman@ime.ac.cn

tion that uses two ball lenses to steer the beam and properly match the different waveguide modes to achieve efficient optical coupling is proposed^[16]. Moreover, Ref.[17] proposed a novel two-lens configuration for the coupling between distributed feedback laser diodes and a silica-based planar lightwave circuit arrayed waveguide grating to relax the lenses assembly requirement. Although these solutions may be able to replace costly and bulky high-precision tools, they increase the difficulty and complexity of chip processing.

In our approach, a novel dual-lens TOSA for DFB laser and a hybrid integration process based on the silicon sub-mount which is a very mature and cost-effective material platform are designed and verified. The dual-lens structure is a combination of a ball lens and an aspherical lens. Simulation results show the positional offsets of the ball lens can be largely compensated by re-aligning the aspherical lens, and both lenses are much tolerant to the misalignment errors. Therefore, to achieve efficient coupling, there is no need to employ expensive and complex high-precision tools, and manufacturing yields can be improved at the same time which will make assembly of each optical system become more cost-effective. In addition, the ball lens is directly fixed onto the hole in the silicon substrate without any mounting structures, so it has great potential for dense integration of multiple channels while maintaining a compact size, which will increase area utilization and reduce cost. The system has been demonstrated with a coupling loss of less than 3 dB between DFB lasers and SMF and a clear eye diagram at 25 Gbit/s.

Fig.1 shows a schematic structure of the TOSA, which mainly comprises six main parts: a silicon sub-mount, a metal substrate, commercial edge emitting DFB lasers (1310D-501 or 1310D-LCT11, Macom) of wavelength around 1 310 nm, a 400- μm -diameter ball lens, an aspherical lens (FBS010Z, IO Solution) and an SMF. Light emitted by the DFB laser is firstly refracted and collected by the ball lens, and the light from the ball lens can be regarded as parallel light. Since the ball lens has different focusing effects on the fast axis and the slow axis of the light, the astigmatism of the beam after compression is more serious, and the spherical aberration of the focused beam is larger, which affects the quality of the beam greatly. When the beam passes through the aspherical lens, the aspherical lens will eliminate and compensate the spherical aberration caused by the ball lens and focuses the light further, thus light convergence and small angle incidence can be achieved.

We have built an optical simulation model in the commercial optical tracing software Zemax to acquire optical transmission characteristic of the system. In Zemax non-sequential mode, DFB laser, ball lens, aspherical lens, and fiber are all properly added and set. Firstly, for DFB laser, the wavelength is set to 1 310 nm, the size of the light-emitting surface is roughly $2\ \mu\text{m}\times 1.5\ \mu\text{m}$, and the maximum divergence angle is $20^\circ\times 18^\circ$. Then radius of curvature, radius/height, aspheric coefficient

and material for the lens are set. Finally, fiber and detection surface are set up. The simulation model in Zemax is shown in Fig.2. By optimizing the distance $S1$ from the laser to the ball lens, the distance $S2$ from the ball lens to the aspheric lens, and the distance $S3$ from the aspherical lens to the fiber, the minimum coupling loss from the laser to the fiber can be obtained as 1.82 dB.

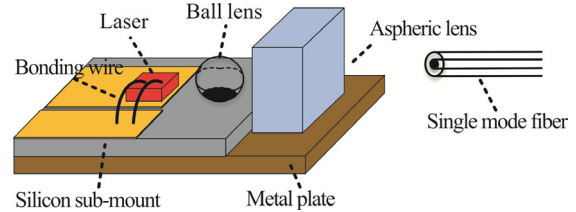


Fig.1 Structure of the dual-lens optical coupling system

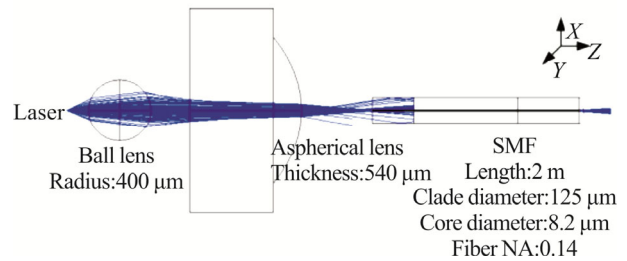


Fig.2 Simulation model of the dual-lens optical coupling system

Comparison between single lens and dual-lens-coupling systems is shown in Tab.1, where DC refers to the direct current laser with a divergence angle of $20^\circ\times 18^\circ$, and AC refers to a high-speed laser with a divergence angle of $40^\circ\times 25^\circ$ that can support 25 Gbit/s. It can be seen the TOSA structure with dual-lens-coupling we designed has better coupling efficiency and more compact footprint, which means smaller form factor and has much potential for dense integration.

Tab.1 Comparison between the coupling systems

System	Laser	Coupling efficiency	Focal length	Ease of assembly
Single aspherical lens	DC	1.94 dB	4 000 μm	Easy (Less optical components)
	AC	2.60 dB	4 000 μm	
Dual-lens	DC	1.82 dB	1 720 μm	Easy (Larger assembly tolerance)
	AC	2.28 dB	1 300 μm	

By changing the position of the lens relative to the x -axis, y -axis, and z -axis, assembly tolerance of the lens in each direction can be evaluated. When the ball lens is offset from its optimal position, coupling performance is shown in Fig.3. The red curve indicates the relative coupling loss of the ball lens as a function of the placement error along the x/y -axis. It can be seen that when the aspherical lens is fixed, the coupling efficiency drops as

much as 1 dB for a $\pm 0.7 \mu\text{m}$ offset from the ideal position which means positional error tolerance is very tight. When offsetting the ball lens and optimizing the position of the aspherical lens at the same time, the black curve in Fig.3 indicates that an offset of $\pm 7 \mu\text{m}$ of the ball lens only degrades the coupling efficiency by 1 dB. This demonstrates that positional errors of the ball lens can be largely compensated by re-aligning the aspherical lens to steer the beam.

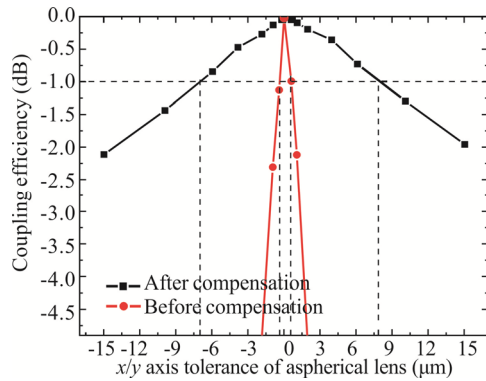


Fig.3 Coupling loss with position offset of the ball lens

On the other hand, if the ball lens is fixed, positional tolerance of the aspherical lens for efficient coupling is shown in Fig.4. We can see an offset of $\pm 4 \mu\text{m}$ on x/y axis of the aspherical lens gives an acceptable relative coupling loss of 1 dB, and the lens is much more tolerant to placement error along z axis. The ball lens has similar tolerance on the vertical axis which is not showed here.

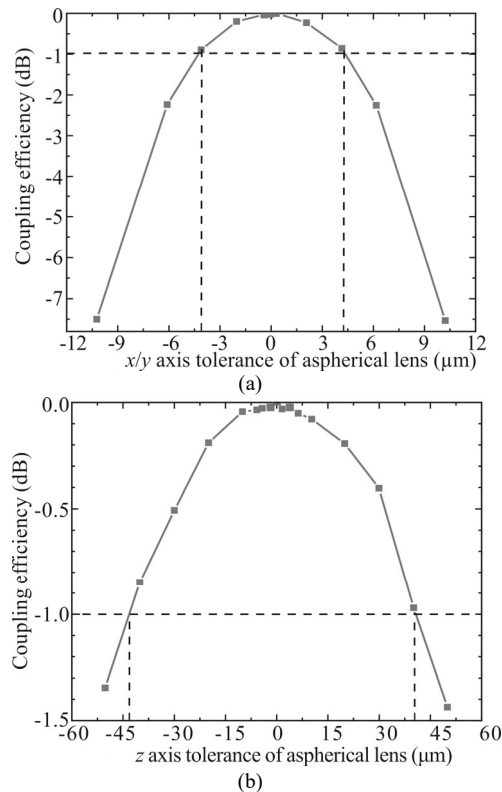


Fig.4 Coupling loss with position offset of the aspherical lens

The TOSA fabrication processes include the assembling of the silicon sub-mount on top of the metal heatsink, surface mounting of the DFB laser and the ball lens on top of the Si bench, and the aspherical lens on top of the mental plate, and wire bonding between the DFB laser and the Si bench. The silicon sub-mount is $390 \mu\text{m}$ thick. Signal integrity is fully considered when designing electrodes and the transmission line for DFB and interconnection on surface of the sub-mount to improve the bandwidth and reduce the electromagnetic radiant cross-talk. In order to position the ball lens accurately, a hole is designed with a diameter of $204 \mu\text{m}$ to make center of the ball lens align with the output light of the laser exactly. The metal substrate is used to place the aspherical lens and protect the assembled silicon sub-mount.

Fig.5 shows the assembly flow diagram of the dual-lens optical coupling structure. Firstly, the DFB die is grasped and placed by Palomar 3800 automatic placement machine. And the attachment to the Si sub-mount is achieved by using conductive silver epoxy. Secondly, the sub-mount assembled with DFB laser is attached to a metal substrate by using thermal conductive epoxy. Subsequently, the ball lens is positioned through the hole on the silicon substrate generally to avoid introducing large post-bonding shifts. Then, the aspherical lens is placed on the metal substrate by using of UV curing epoxy and adjusted to find the best coupling position. Finally, the electrode pads of DFB are connected to the silicon sub-mount by wire bonding. Fig.6 shows a photograph of the assembled TOSA system with an inset of the silicon sub-mount under a microscope.

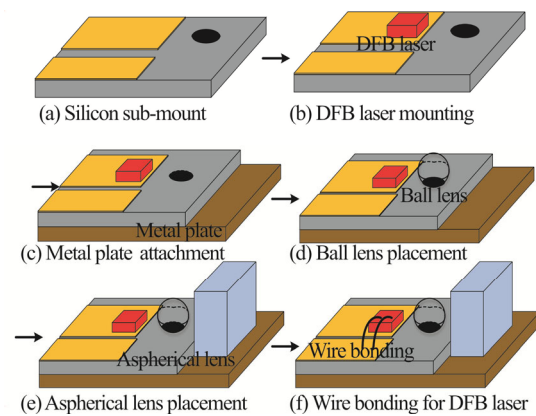


Fig.5 Assembly flow diagram of the TOSA

To better verify the $L-I$ characteristics of the laser coupled into the SMF, we assembled and tested the DC laser (MACOM 1310D-501) with a narrower beam divergence angle $20^\circ \times 18^\circ$ firstly. As shown by the solid line in Fig.7, the output power at 40 mA injection current is 3.8 mW and threshold current of the DC DFB laser is about 10 mA. Assuming the ramp efficiency of 0.4 mW/mA, then the emitting power from the laser at 40 mA is estimated to be 12 mW. Therefore, the total loss can be calculated to be 4.99 dB. The dotted line in Fig.7

presents the L-I characteristics of the AC laser coupled into the fiber with a beam divergence angle of $40^\circ \times 25^\circ$, the coupling loss can be calculated by the same method as 6.2 dB, which is much bigger than coupling loss of the DC laser. This is because ball lens of the same diameter has a smaller converging effect on the beam with a large divergence angle. It should be noted that when calculating the coupling efficiency, the transmission loss of the single-mode fiber, the connect loss of the optical power meter, and also the inherent DFB loss are included. By subtracting the additional losses and considering the actual output fraction of laser light, the coupling efficiency of the dual-lens TOSA is estimated to be less than 3 dB. We believe the discrepancy of coupling efficiency between simulation and experiment results from DFB bonding accuracy, fixed accuracy from the machine for assembly, and manual error of fiber alignment.

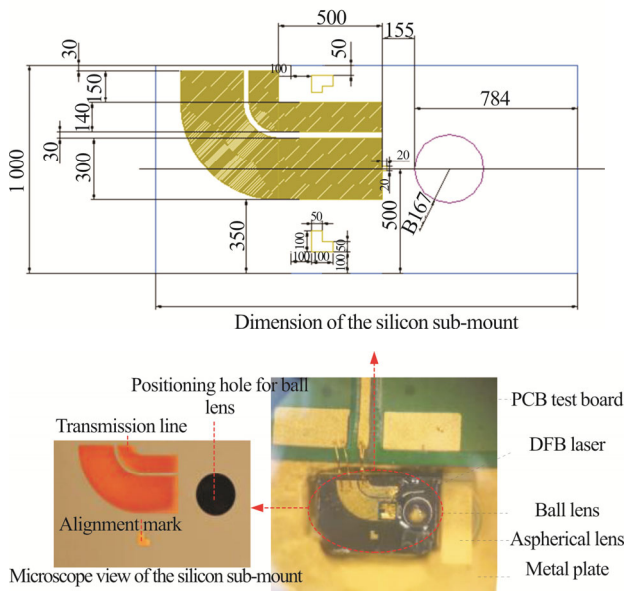


Fig.6 Photograph of the assembled coupling system

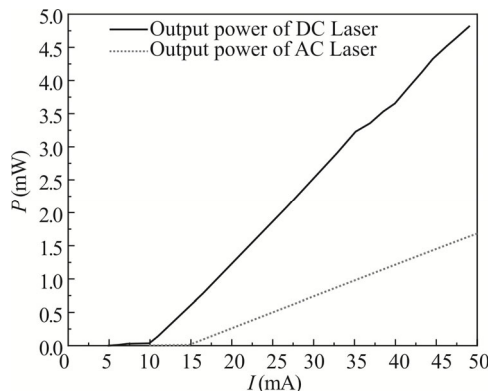


Fig.7 Output power of the DFB lasers coupled to fiber as a function of injection current

Eye diagram under 10 Gbit/s and 25 Gbit/s are tested to verify high-speed transmission performance of the

TOSA. Schematic diagram and test results of the optical eye diagram measurement are shown in Fig.8 and Fig.9. Clear eye openings are obtained, which has extinction ratio of 3.2 dB and 4.5 dB, respectively. We believe there is still space to significantly improve the system's high-speed performance by further optimizing the interconnect bandwidth of the test board.

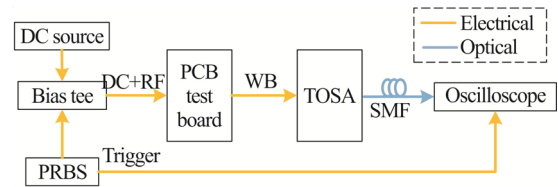


Fig.8 Schematic diagram of the high-speed performance measurement setup

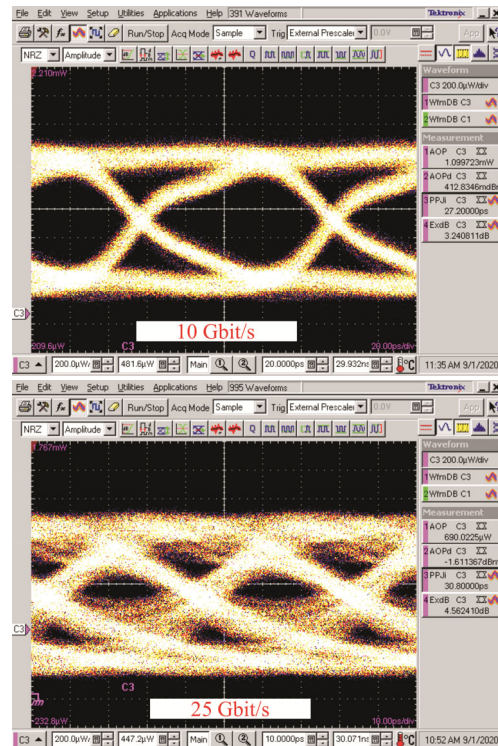


Fig.9 Measured optical eye diagram at 10Gbps and 25Gbps

We have demonstrated a cost-efficient and compact TOSA module based on hybrid integration in the O band. The dual-lens is horizontally coupled to the DFB laser. A silicon carrier is used to connect the DFB laser with external circuit, which is optimized for high-speed transmission performance. The system is much smaller compared to conventional single lens system and has larger position tolerance. Besides, the system does not require much precision on equipment used to assemble which means higher yield and lower cost. The fabricated TOSA module has clearly opening eyes with minor time jitters at a baud rate of 25 GBaud. This hybrid integration is a

low fabrication cost, compact, and low insertion loss method, providing a potential solution for small-size and multi-channel optoelectronic subassembly explored DFB lasers in a high-speed optical network.

References

- [1] Qixiang Cheng, Meisam Bahadori, Madeleine Glick, Sébastien Rumley and Keren Bergman, *Optica* **5**, 1354 (2018).
- [2] Lianping Hou, Mohsin Haji, Jehan Akbar, John H Marsh and A Catrina Bryce, *Optics Letters* **36**, 4188 (2011).
- [3] Aruga Hiroshi, Mochizuki Keita, Muraio Tadashi and Shirao Mizuki, *IEICE Transactions on Electronics* **E102-C**, 324 (2019).
- [4] Takaharu Ohyama, Yoshiyuki Doi, Wataru Kobayashi, Shigeru Kanazawa, Kiyoto Takahata, Atsushi Kanda, Takeshi Kurosaki, Takuya Tanaka, Tetsuichiro Ohno, Hiroaki Sanjoh and Toshikazu Hashimoto, *Journal of Lightwave Technology* **34**, 1038 (2016).
- [5] Takaharu Ohyama, Yoshiyuki Doi, Wataru Kobayashi, Shigeru Kanazawa, Takuya Tanaka, Kiyoto Takahata, Atsushi Kanda, Takeshi Kurosaki, Tetsuichiro Ohno, Hiroaki Sanjoh and Toshikazu Hashimoto, *IEEE Photonics Technology Letters* **28**, 802 (2016).
- [6] Bardia Pezeshki, John Heanue, Dinh Ton, Thomas Schrans, Suresh Rangarajan, Sarah Zou, Gideon W. Yoffe, Alice Liu, Michael Sherback, Jay Kubicky and Paul Ludwig, *Journal of Lightwave Technology* **32**, 2796 (2014).
- [7] Jun-Ming An, Jia-Shun Zhang, Liang-Liang Wang, Kaiwu Zhu, Bingli Sun, Yong Li, Jie Hou, Jian-Guang Li, Yuan-Da Wu, Yue Wang and Xiao-Jie Yin, *Optical Engineering* **57**, 1 (2018).
- [8] Y. Gao, C. Bolle, Y. Low, R. Papazian, M. Cappuzzo, B. Keller, F. Pardo and M. P. Earnshaw, *IEEE Photonics Technology Letters* **28**, 2549 (2016).
- [9] Xing Jiyao, Rong Weibin, Sun Ding, Wang Lefeng and Sun Lining, *Applied Optics* **55**, 6947 (2016).
- [10] Jiang Jinhong, Li Yongqi, Lu Huanzhu, Jin Qi and Zhang Kefei, *Laser Technology* **43**, 655 (2019). (in Chinese)
- [11] Che-Hsin Lin, Szu-Chin Lei, Wen-Hsuan Hsieh, Ying-Chien Tsai and Wood-Hi Cheng, *Optics Express* **25**, 24480 (2017).
- [12] Kwon-Seob Lim, Hyoung-Jun Park, Hyun Seo Kang, Young Sun Kim and Jae-Hyung Jang, *Optical Engineering* **55**, 026107 (2016).
- [13] Takaharu Ohyama, Yoshiyuki Doi, Wataru Kobayashi, Shigeru Kanazawa and Toshikazu Hashimoto, *Journal of Lightwave Technology* **34**, 1038 (2016).
- [14] Hoque Muttahid-Ull, Hasan Md Nazmul and Lee Yung-Chun, *Sensors and Actuators A: Physical* **254**, 36 (2017).
- [15] Takanori Suzuki, Koichiro Adachi, Aki Takei, Kohichi R. Tamura, Akira Nakanishi, Kazuhiko Naoe, Tsukuru Ohtoshi, Kouji Nakahara, Shigehisa Tanaka and Kazuhisa Uomi, *Journal of Lightwave Technology* **34**, 358 (2016).
- [16] Y. Gao, C. Bolle, Y. Low, R. Papazian, M. Cappuzzo, B. Keller, F. Pardo and M. P. Earnshaw, *IEEE Photonics Technology Letters* **28**, 2549 (2016).
- [17] Liu Jun, Huan Qingzhong and Xia Jinsong, *IEEE Photonics Journal* **11**, 1 (2019).